Fermi National Accelerator Laboratory

FERMILAB-Conf-82/49-EXP
7550.537

J/ψ RESONANCE PRODUCTION IN 125 GeV/c $\bar{p}N$ AND $\pi^- N$ INTERACTIONS*

E. Anassontzis, S. Katsanevas, P. Kostarakis, C. Kourkoumelis, A. Markou, L. K. Resvanis, and G. Voulgaris
University of Athens, Athens, Greece

and

M. Binkley, B. Cox, J. Enagonio, C. Hojvat, D. Judd, R. D. Kephart, P. K. Malhotra, P. O. Mazur, C. T. Murphy, F. Turkot, R. L. Wagner, D. Wagoner, and W. Yang
Fermi National Accelerator Laboratory, Batavia, Illinois 60510 USA

and

H. Areti, S. Conetti, P. Lebrun, D. Ryan, T. Ryan, W. Schappert, and D. Stairs
McGill University, Montreal, Canada

and

C. Akerlof, P. Kraushaar, D. Nitz, and R. Thun
University of Michigan, Ann Arbor, Michigan 48104 USA

and

He Mao, Zhang Nai-jian
Shandong University, Jinan, Shandong, Peoples Republic of China

July 1982

ABSTRACT

We present preliminary results for the production of the J/ψ resonance in 125 GeV/c antiproton and pi minus-nucleon interactions as determined from an analysis of 9100 antiproton and 28750 pi minus induced J/ψ's. Total cross sections ($x_F > 0$) for J/ψ production by both particle types are determined and the ratio of $\sigma_{\bar{p}}/\sigma_{\pi^-}$ is found to be 0.88 ± 0.05. Differential cross sections for J/ψ production are given as a function of x_F and p_T. The ratio of the $\frac{d\sigma}{dx_F}$ cross sections as a function of x_F is shown.

---

*Presented at the XXI International Conference on High Energy Physics, Paris, France, July 26-31, 1982.

In experiment E-537 recently performed in the High Intensity Laboratory in the Proton Area at Fermilab, we have measured J/ψ production (by means of detection of the $J/\psi \rightarrow \mu^+\mu^-$ decays) in $\bar{p}W$ and π^-W interactions at 125 GeV/c. A special enriched antiproton beam[1,2] produced from $\bar{\Lambda}^o \rightarrow \bar{p}\pi^+$ decay was used in this experiment. With this beam we were able to obtain 2×10^6 $\bar{p}$ and 8×10^6 π^-/sec at 125 GeV/c when operating with a 5×10^{12}/sec,400 GeV/c proton beam. The identity, momentum and trajectory of the incident beam particles were tagged by a system consisting of two 21 meter differential Cerenkov counters, two bending magnets and three PWC and scintillator hodoscope stations. This system measured momentum to $\sim$ 1% and tagged beam particle identity with only 1% contamination of the antiproton flux while operating routinely at 10^7 particles per second.

The large acceptance forward spectrometer (shown in Fig. 1) which was used to collect the data has been described elsewhere[2] and will only be described briefly here. The decay muons from J/ψ's produced in a 1.0 or 1.5 interaction length W target passed through a 149 cm copper hadron absorber and were measured in a set of 9 drift chamber planes just upstream of the 91 cm x 183 cm, 27.7 kG meter analysis magnet of the spectrometer. An additional measurement to improve mass resolution by improving the measurement of the opening angle of the muons was performed by a set of proportional wire planes

embedded in the copper absorber. The trajectories of the muons downstream of the magnet were measured by 12 planes of drift chambers. Finally the muons were required to penetrate 1.8 meters of steel and 0.9 meters of high density concrete and make a muon triple coincidence in the three large hodoscope planes of the muon detector.

The fast logic trigger for the J/ψ dimuons consisted of an identified beam particle (either $\bar{p}$ or π^-), two or more muon hodoscope triple coincidences in different quadrants of the spectrometer, and at least two particles detected in the large charged particle hodoscope just downstream of the last drift chamber set. A wall of veto counters positioned just upstream of the spectrometer was used to veto muon halo. A more restrictive trigger was sometimes imposed which required, in addition, at least one penetrating particle outside a 15 cm radius at the downstream end of the copper absorber. The quadrant of this penetrating particle was required to be the same as the quadrant of one of the muon triple coincidences.

In addition to the fast logic, a trigger processor[3] was prepared for the experiment which used the modular ECL CAMAC system developed at Fermilab. This processor searched the rear drift chamber x planes for tracks in regions (roads) defined by the triple coincidences under the assumption that all muons came from the target. The system then determined angles and momenta for all tracks that were found and

calculated the invariant mass of all pairs of tracks. If any pair had a mass greater than 2 GeV/c^2, the event was recorded. The mass resolution possible with the trigger processor, while much cruder than the achievable off-line mass resolution for the completely reconstructed event (using the drift chamber time information), was adequate such that the 2 GeV/c^2 mass cut caused a loss of less than 1.0% of the accepted J/ψ's which triggered the fast logic.

The acceptance for the J/ψ's has been calculated for the spectrometer by a Monte Carlo procedure which incorporated geometric efficiencies, energy loss, multiple scattering, fast trigger cuts and trigger processor cuts. These acceptances in x_F and p_T assumed flat cos θ^* and ϕ^* distribution. θ^* is the angle of a decay muon with respect to the beam in the dimuon center of mass system and ϕ^* is the azimuthal angle in the same system (Gottfried-Jackson frame). The spectrometer has good acceptance for J/ψ in the entire forward hemisphere ($x_F > 0$) and essentially flat p_T acceptance in the p_T range of the measurement.

The mass spectrum for the region $2.5 < M_{\mu^+\mu^-} < 5.0$ GeV/c^2 is shown in Fig. 2 for $\bar{p}W \rightarrow \mu^+\mu^- + X$. The J/$\psi$ signal dominates the spectrum with the ψ' appearing as a shoulder. The ratio of ψ' to J/ψ production was extracted by fitting two gaussians centered at 3.1 and 3.7 GeV/c^2 and an exponential background to the data of Fig. 2. The $\sigma \cdot B(\psi')/\sigma \cdot B(\psi)$ was determined to be 0.029 ± 0.007 for the antiproton data. The same technique

applied to our π^- data yielded a ratio of 0.029 ± 0.004. The preliminary values for total cross sections ($x_F > 0$) for J/ψ production by 125 GeV/c antiprotons and pi minus are $\sigma_{\bar{p}} = 50.7 \pm 1.0 \pm 10.1$ nb/nucleon and $\sigma_\pi = 57.7 \pm 0.6 \pm 11.5$ nb/nucleon. These cross sections were derived using the branching ratio, $B(\psi \to \mu^+\mu^-) = 0.07$[4] and an A dependence of the form $\sigma = \sigma_o A^{0.93}$ from a collection of world data compiled by Lyons.[5] The first of the two quoted errors on each cross section is the statistical error and the second number is our current estimate of the systematic error. The study of the sources of the systematic error is underway and we expect this error to decrease significantly.

Using these cross sections we obtain a ratio of J/ψ production ($x_F > 0$) in $\bar{p}N$ interactions to that in π^-N interactions at 125 GeV/c of 0.88 ± 0.05 (systematic errors included). In order to calculate the ratio of proton to antiproton production of J/ψ at this momentum, $\sigma_p/\sigma_{\bar{p}}$, we have used a parameterization of proton induced J/ψ cross section data by Lyons[5] of the form $\sigma = 850\, e^{-17\sqrt{\tau}}$ nb/nucleon ($x_F > 0$, $\sqrt{\tau} = M/\sqrt{s}$). In this way we obtain a $\sigma_p = 27.4$ nb/nucleon which gives a ratio $\sigma_p/\sigma_{\bar{p}} = 0.54 \pm 0.11$ (only the error from our antiproton data is included). In Fig. 3a and 3b we show our values for these ratios along with the values measured at other energies by the Omega[6] and NA3[7] collaborations. The antiproton to pion ratio is remarkably constant over a large energy range while the proton to antiproton

ratio markedly increases from values near 0.2 at $s = 100$ GeV^2 to almost 0.7 at $s = 400$ GeV^2. The curves in Figs. 3a and b are QCD predictions for the s dependence of these ratios. The solid curves are from a model by Glück, Owens, and Reya[8] which contains contributions to J/ψ production from the $q\bar{q} \to c\bar{c}$ and $gg \to c\bar{c}$ processes. The dashed curve of Fig. 3b is the calculation from a model of Carlson and Suaya[9] in which J/ψ's are produced through an intermediate P-wave charmonium χ state with the subsequent decay of the $\chi \to \psi\gamma$. Both models describe the s dependence of these ratios reasonably well. The major inference that can be drawn is that the gluon-gluon processes are necessary to explain the s-dependence of the data.

The p_T distributions for our antiproton and pion data are shown in Fig. 4. The pi minus distribution is flatter than that of the antiproton distribution. The average p_T^2 is larger for the pi minus induced J/ψ's ($\langle p_T^2 \rangle_{\pi^-} = 1.45 \pm 0.02$) than for the antiproton induced J/ψ's ($\langle p_T^2 \rangle_{\bar{p}} = 1.23 \pm 0.03$). Both data sets fit well the empirical form, $\frac{1}{p_T} \frac{d\sigma}{dp_T} \sim (1 + \frac{p_T^2}{M^2})^{\alpha}$. The parameters for the fits shown in Fig. 4 are:

$$\alpha_{\bar{p}} = -9.0 \pm 0.9 \qquad \alpha_{\pi^-} = -8.6 \pm 0.5$$

$$M_{\bar{p}} = 2.95 \pm 0.19 \qquad M_{\pi^-} = 3.08 \pm 0.13$$

Both p_T distributions are quite steep and the value of M is near the J/ψ mass for both data sets.

The x_F distributions for the antiproton and pion data are shown in Fig. 5. There are striking differences between the pion and antiproton induced J/ψ. This behavior is similar to the behavior of our pion and antiproton high mass ($M > 4$ GeV/c^2) dimuon data reported elsewhere[2] in this conference. We have fitted these data to a gaussian form $\frac{d\sigma}{dx_F} \sim e^{-(x-a)^2/2\sigma^2}$ and find

$$a_{\bar{p}} = 0.018 \pm 0.015 \qquad a_{\pi^-} = 0.14 \pm 0.01$$

$$\sigma_{\bar{p}} = 0.23 \pm 0.01 \qquad \sigma_{\pi^-} = 0.28 \pm 0.01$$

The pion data peaks at $x_F > 0$ and is broader than the antiproton distribution. Finally, we have calculated the ratio $(\frac{d\sigma}{dx_F})_{\bar{p}N\to\psi X} / (\frac{d\sigma}{dx_F})_{\pi^-N\to\psi X}$ as a function of x_F. This is shown in Fig. 6 along with 200 GeV/c data from the NA3 experiment. The errors are statistical. At small x_F the ratio from our 125 GeV/c data is steeper and greater in magnitude than the 200 GeV/c data. The curve is a 200 GeV/c prediction for this ratio from a color evaporation model by Barger, Keung, and Phillips[10] for J/ψ production via $gg \to J/\psi$ and $q\bar{q} \to J/\psi$. The x_F dependence of this prediction appears to match our data well above x_F of 0.2 but falls considerably below the data for $x_F < 0.2$.

In conclusion, we have measured J/ψ production in 125 GeV/c antiproton and pi minus-tungsten interactions. We find the antiproton and pi minus cross sections nearly equal and considerably larger than the proton cross section. The behavior of the ratio

of these cross sections implies large gg contributions when interpreted in the context of the currently available models of J/ψ production. The p_T distribution for the antiproton induced J/ψ's is steeper than that of the pi minus induced J/ψ's. The x_F distributions for the two reactions are quite different with the pi minus distribution shifted to $x_F > 0$ and broader than the antiproton distribution suggesting a more energetic constituent composition in the pion.

We wish to thank the personnel of the Fermilab Proton Department and the Fermilab Physics Section for their support over the course of this experiment. We would also like to thank the U.S. Department of Energy, the National Science Foundation-International Programs and -High Energy Physics Divisions, the Natural Sciences and Engineering Research Council of Canada, Quebec Department of Education, and the Hellenic Science and Technology Agency for their support.

REFERENCES

1. B. Cox, Fermilab Report 79/1, 0090.01, January (1979).

2. Production of Muon Pairs with Masses Greater than 4 GeV/c^2 in $\bar{p}N$ and $\pi^- N$ Interactions at 125 GeV/c, submitted to the XXI International High Energy Physics Conference, Paris, France (1982).

3. P. Kostarakis, et al., Topical Conference on the Application of Microprocessors to High Energy Physics Experiments, CERN, 4 May 1981.

4. N. Barash-Schmidt, et al., Reviews of Mod. Phys., 52 , (1980).

5. L. Lyons, Oxford NP-80/80 (1980).

6. M. J. Corden, et al., Phys. Lett. 96B, 417 (1980).

7. J. Badier, et al., NA3 Collaboration, CERN/EP 79-61 (1979).

8. M. Glück, J.F. Owens and E. Reya, Phys. Rev. 17D, 2324 (1978).

9. C.E. Carlson and R. Suaya, Phys. Rev. 18D, 760 (1978).

10. V. Barger, W.Y. Keung and R.J.N. Phillips, Zeitschrift für Physik C, 6, 169 (1980).

FIGURE CAPTIONS

Fig. 1 E-537 spectrometer.

Fig. 2 Dimuon mass in the region $2.5 < M_{\mu^+\mu^-} < 5.0$ GeV/c^2. The dotted curve is the extrapolation of a fit to the exponential background under the ψ and ψ'.

Fig. 3a The ratio of the total cross sections $\sigma(\bar{p}N \to \psi x)/\sigma(\pi^- N \to \psi x)$ as a function of s.

Fig. 3b The ratio of the total cross sections $\sigma(pN \to \psi x)/\sigma(\bar{p}N \to \psi x)$ as a function of s. The solid curves are a direct gluon and quark fusion model for J/ψ production. The dotted curve is a model in which J/ψ proceeds through the production of intermediate χ's.

Fig. 4 $\frac{1}{p_T}\frac{d\sigma}{dp_T}$ vs. p_T for $\bar{p}N \to \psi x$ and $\pi^- N \to \psi x$ (for $x_F > 0$).

Fig. 5 $\frac{d\sigma}{dx_F}$ vs. x_F for $\bar{p}N \to \psi x$ and $\pi^- N \to \psi x$. The curves are the fit $e^{-(x-a)^2/2\sigma^2}$ discussed in the text.

Fig. 6 Preliminary ratio of $\frac{d\sigma}{dx_F}(\bar{p}N \to \psi x)/\frac{d\sigma}{dx_F}(\pi^- N \to \psi x)$ vs. x_F for our 125 GeV/c data. The solid curve is the prediction of the dependence of this ratio on x_F at 200 GeV/c. The 200 GeV/c NA3 experimental data are also shown.

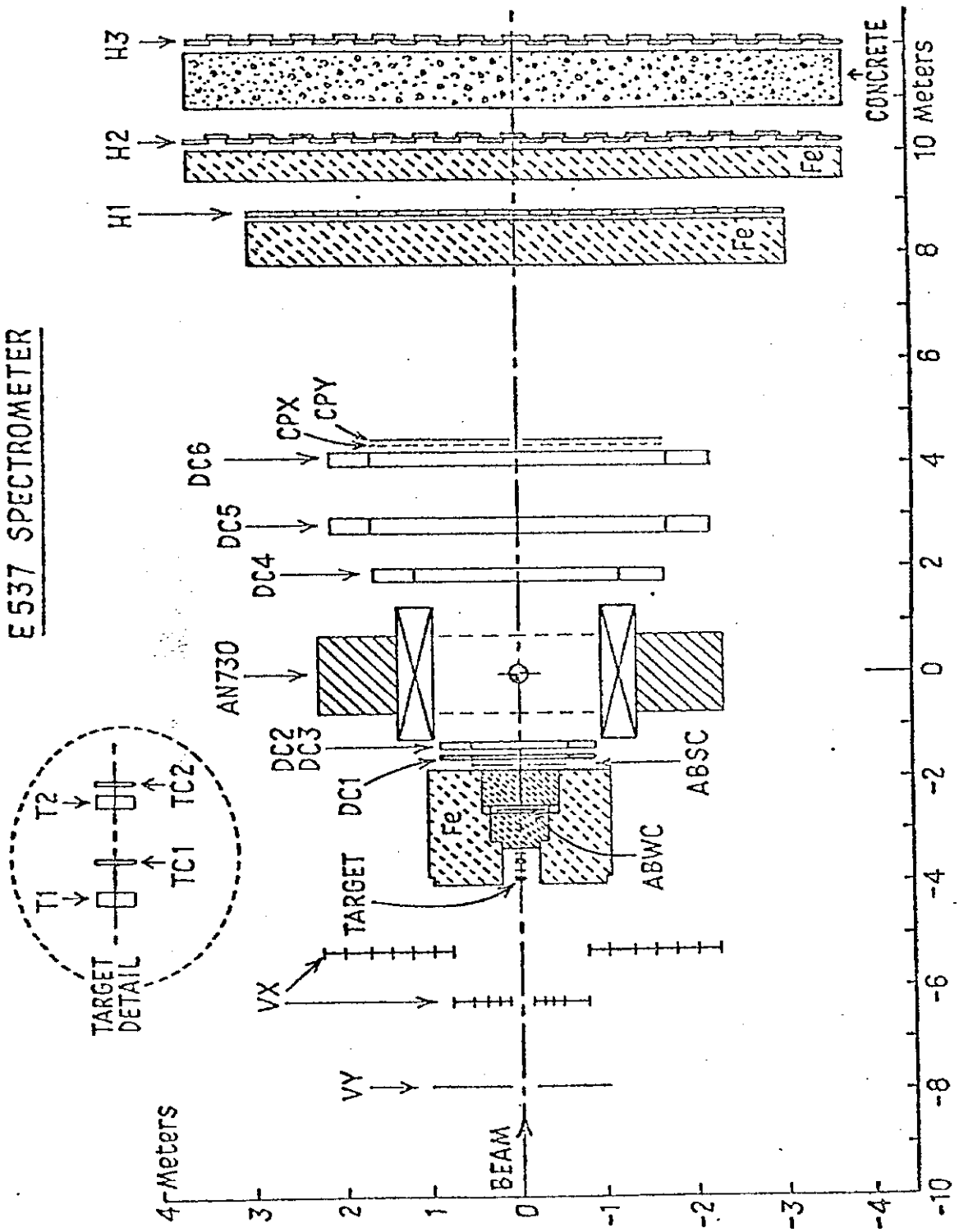
E537 SPECTROMETER
H3
H2
H1
Fe
CONCRETE
10 Meters
DC6
CPX
CPY
DC5
DC4
AN730
DC2
DC3
DC1
ABSC
ABWC
TARGET
VX
VY
BEAM
4 Meters
TARGET DETAIL
T1
T2
TC1
TC2

FIG. 1

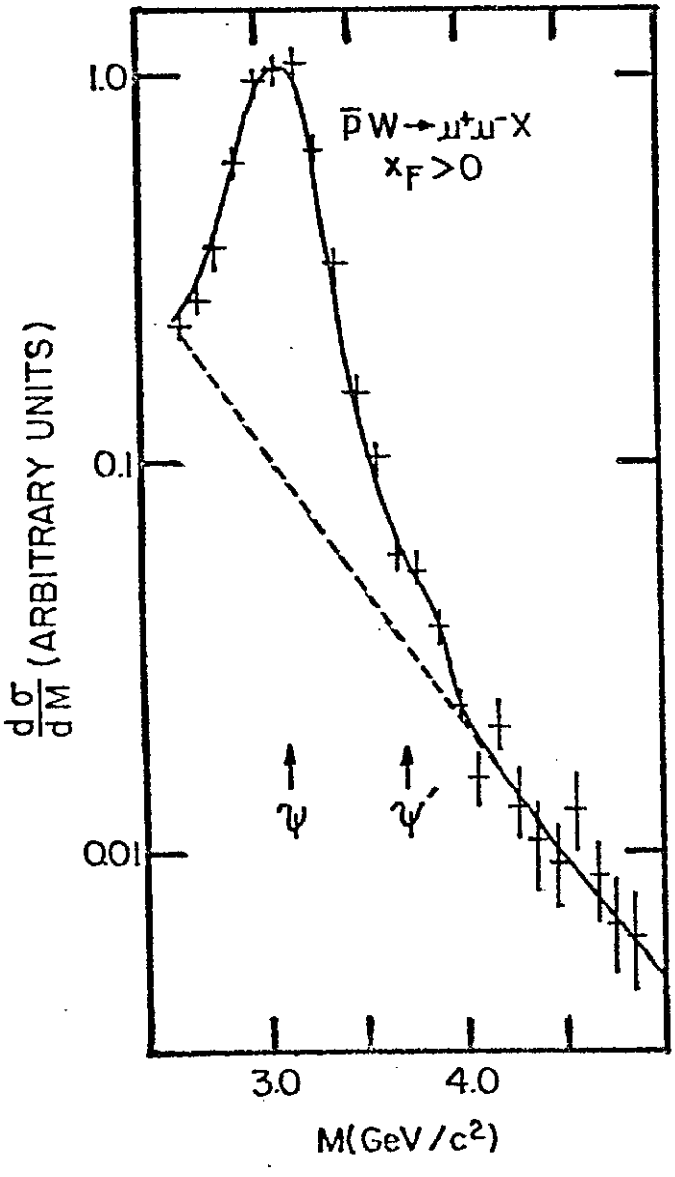
1.0
0.1
0.01
$\bar{p}W \rightarrow \mu^+\mu^- X$
$x_F > 0$
$\frac{d\sigma}{dM}$ (ARBITRARY UNITS)
ψ
ψ'
3.0
4.0
M(GeV/c^2)

FIG. 2

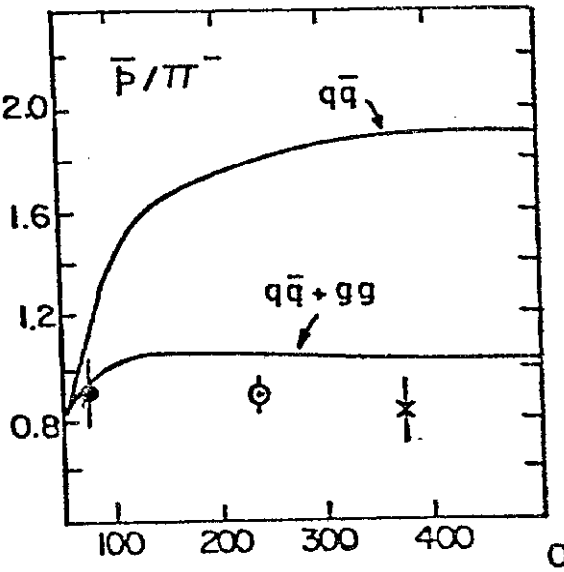
$\bar{p}/\pi^-$
$q\bar{q}$
$q\bar{q}+gg$
2.0
1.6
1.2
0.8
100
200
300
400

FIG. 3a

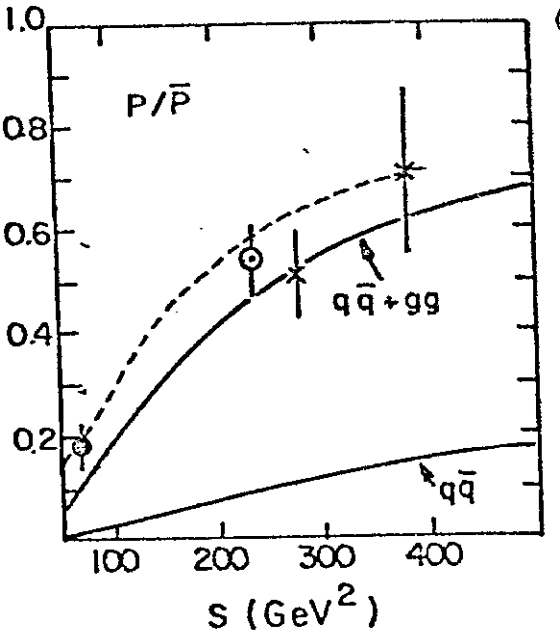
$\sigma_{TOT}(\psi)_{x_F>0}$ RATIOS
⊙ E 537
● Ω
x NA 3
$p/\bar{p}$
$q\bar{q}+gg$
$q\bar{q}$
1.0
0.8
0.6
0.4
0.2
100
200
300
400
S (GeV^2)

FIG. 3b

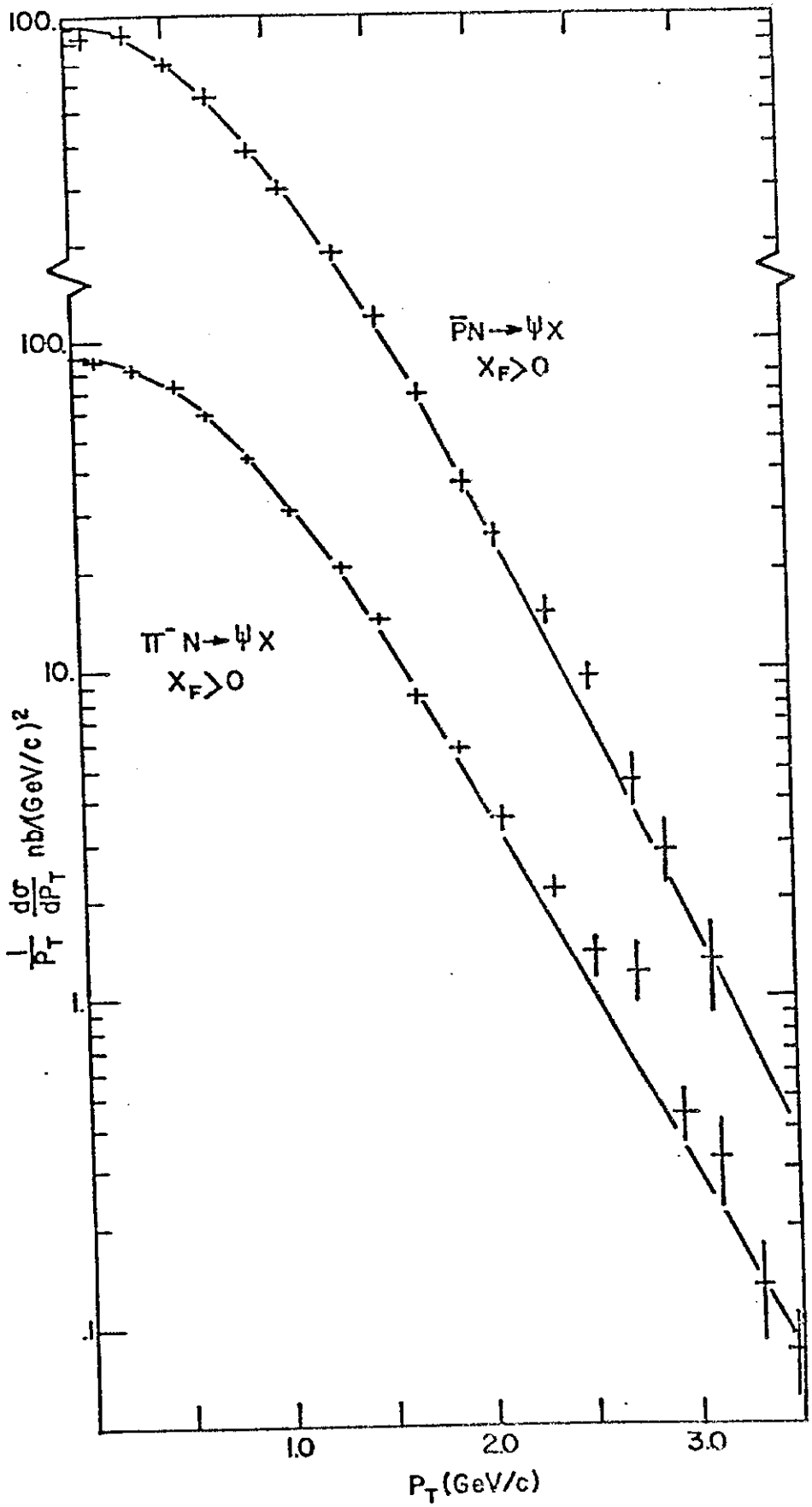
100.
100.
10.
1.
.1
$\bar{P}N \rightarrow \psi X$
$X_F > 0$
$\pi^- N \rightarrow \psi X$
$X_F > 0$
$\frac{1}{p_T} \frac{d\sigma}{dP_T}$ nb/(GeV/c)^2
1.0
2.0
3.0
P_T(GeV/c)

FIG. 4

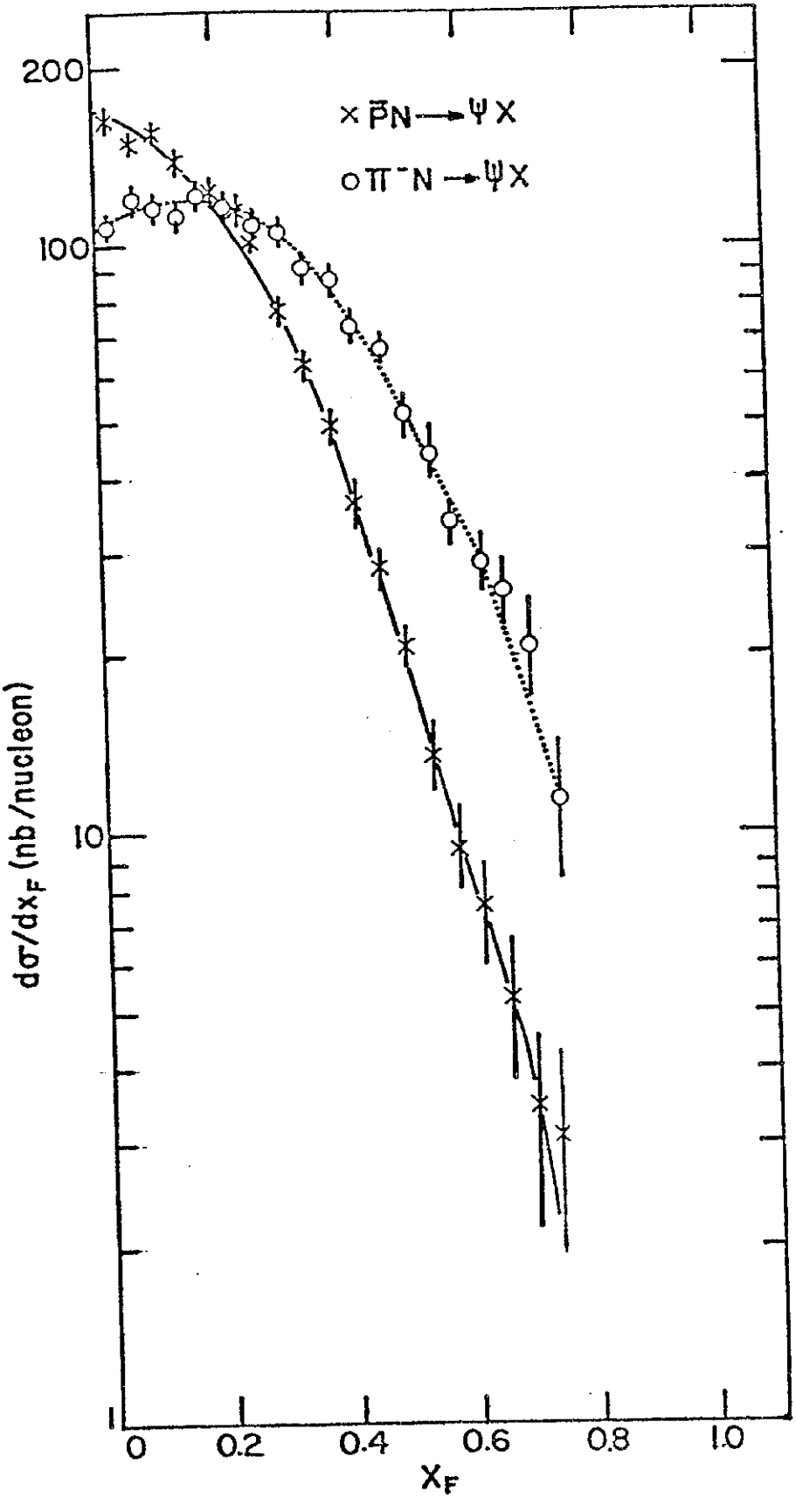

FIG. 5

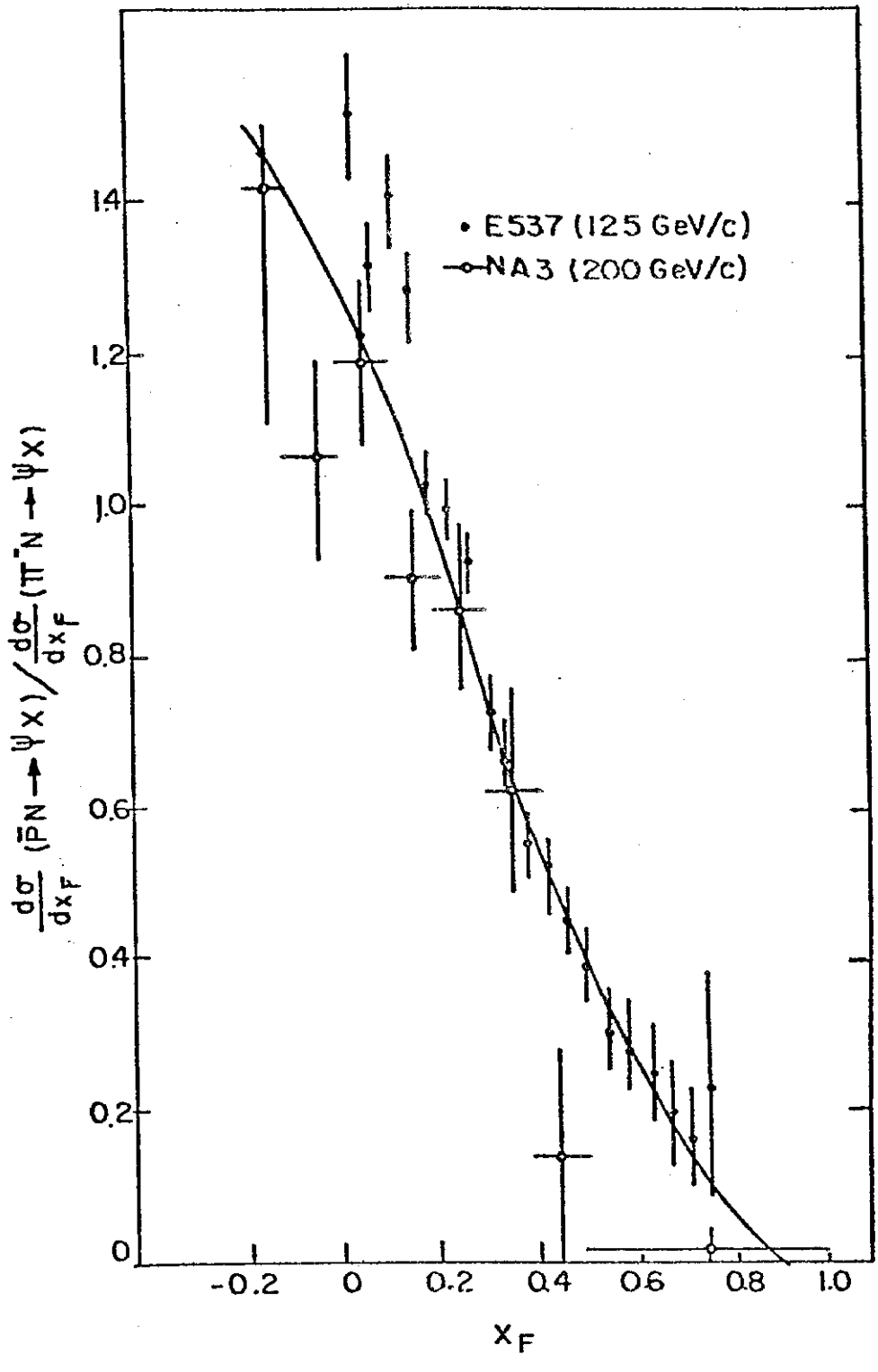
• E537 (125 GeV/c)
NA3 (200 GeV/c)
$\frac{d\sigma}{dx_F}(\bar{p}N \to \psi X) / \frac{d\sigma}{dx_F}(\pi^- N \to \psi X)$
1.4
1.2
1.0
0.8
0.6
0.4
0.2
0
-0.2
0
0.2
0.4
0.6
0.8
1.0
x_F

FIG. 6